BBMS: Investigation to Single Colour Image Visibility Improvement in Turbid Media through Biorthogonal Wavelet Based Depth-map Estimation

Sangita Roy[1]

ECE Department Narula Institute of Technology, Kolkata, India

[1] ORCID: 0000-0002-8898-0183, roysangita@gmail.com

Abstract

Electronic imaging needs good quality, high resolution (HR) digital images for highlighting finer details of the image. Normally images captured by ordinary digital camera are post pro cessed with available software instead of high cost CMOS sensor phased camera. Problem commonly faced with these images may get degraded due to the scattering media which deteriorates contrast, shifts colour, and make overall image whitish. Information from the distant objects suffer from poor medium transmission as well as noise amplification. Biorthogonal wavelet denoising (BWD), compress sparsely in frequency -time space, removes noise from depth estimation and makes the transmission smooth. Moreover, single image recovery is a serious challenge and ill posed problem. The recovered image improves compare to degraded image significantly and dis cards possibility of false edge detection as well as prevent colour shift and low contrast. Good quality images are found with objective evaluation. Moreover, different wavelets, thresholds, and decomposition levels have been studied and compared. Time complexity is linear due to wavelet domain analysis which makes the technique fast, reliable, and visually pleasing.

Keywords: Biorthogonal wavelet, denoising, image recovery model, scattering media, dehazing, Quality Assessment, IQA (Image Quality Assessment).

1. Introduction

Electronic imaging applications require good quality image or video with HR (High Resolution). HR defines as high pixel density. Since 1970s CCD (Charge Coupled Device) and CMOS sensor based digital cameras are being used for digital images. But current trends in HR and corresponding price are sometimes beyond reach of common people or for commercial applications. In such cases post processing is the only solution with the help of available software. These software or techniques not only increase resolution but also removes blur and noise that come along with natural images in scattering media in the form of haze, mist, dust, fog etc [1,2]. The above-mentioned effects make the look of digital images low contrast, colour shifting, whitish, dull and blur. This problem is so serious that during 2000-2018 thousand of research papers produced to meet the challenges. Surprisingly this challenge is partially solvable due to the suspended solid as well as liquid particles in the environment which are increasing alarmingly and leading to global environ mental pollution. In such conditions, clear information from the degraded digital images or video are of high demand in the area of surveillance, navigation, machine vision, oceanography, flight safety, etc [3]. Several post processing techniques are available with high as well as low computational complexity. It is also obvious that more complex techniques will revive artifact-free image accurately with good contrast, colour, and bright ness. But in some cases, low complexity or fast visibility improvement of digital images are needed. Lot of re searches are focusing on low complexity vis-

ibility improvement. Authors are focusing on this area since long. This problem encompasses dehazing, defogging, deraining, desmogging etc. The recovery problem is ill-posed inverse in nature. The solution of this type of problem is not exact, rather depends on estimation or prediction on the parameter or parameters. The difference between exact to predict parameters estimation as less as possible makes the technique efficient. Therefore, there is always newer way to estimate those variables to get back original information which somehow unachievable through normal enhancement procedure. Image enhancement, Image Fusion, and Image Restoration are the three basic dehazing methods. Image enhancement based dehazing are not very well known due to its inability to reproduce visibility. Contrast and visibility improve partially. Image fusion based dehazing requires multiple channel images to construct high quality image. It has no need for any physical model. that multiple channel source information sometimes difficult to collect. Image restoration based dehazing employs physics based optical image formation model. Original image radiance is retrieved by inverting the model and estimating some parameters which cause the distortion. This restoration based dehazing are three types: a) Additional Information based, b) Multiple image, and c) Prior knowledge based [3]. **Contribution** The proposed method is based on prior knowledge physics based optical image formation model. This technique requires single image which is the uniqueness and effectiveness of the technique. Retrieval of the original radi ance solely depends on estimation of few parameters. This is the main challenge. Blur and Noise are the two sources of disturbances of this technique which adhere to the pixels exponentially as they move from source to destination and within the acquiring device respectively. Noise amplifies during inversion of the image recovery is highly challenging subject. The nature of haze is neither uniform or nor global, rather local and scene radiance decays exponentially, and resulting image blurring at the receiving end. While noise is statistically random and additive in nature. As a result, far objects are affected more than nearby objects. Some state-of-the art algorithms of the single image dehazing are the work of Tan [4], Fattal [5], He [6], Tarel [7], Berman [8], and Roy [32,33, 34].

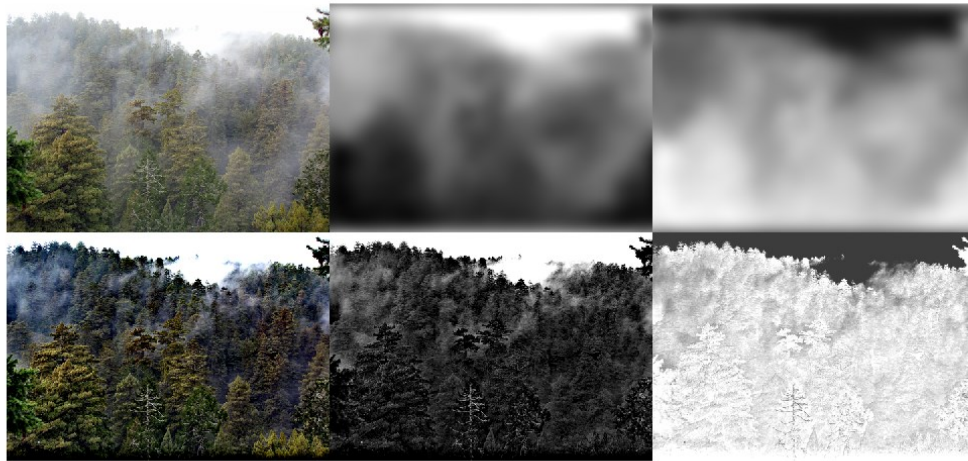Example of Natural outdoor Image

Fig. 1. a) Sample hazy image with its depth map, transmission estimation (b) Dehazed image with its Depth map, Transmission estimation

The rest of this paper is arranged as follows. In Section II, different eminent researchers in this field have been studied. Image formation model has been discussed with mathematical details in section III. In section IV, Biorthogonal Wavelets has been examined in detail. In V Application of Biorthogonal Wavelets in Image recovery model has been justified. In VI Image Quality assessment with related quality assessment criteria of dehazing algorithms has been described. VII Result of experiment performed are furnished. In section VIII application

of the technique on different degraded images with result has been shown. Finally, in IX conclusions and shortcomings of the work has been presented with future research directions.

2. Work of Eminent previous researchers in this field

Single image dehazing is under-constrained problem. Under this class, prior knowledge based de hazing is of high potential and newer algorithms are coming up fast with great promise. Our work is based on prior knowledge based single image dehazing. The important research work under this class is enumerated below. **Okley *et al.*'s** [9] in 1998: day light image, scattered by aerosol with attenuation as each pixel travels with distance from the radiance point to sensor. The model used was the physics based inverse model of H Kosmeider[10] and improved by J Marcartney[11]. Sig nal-to-noise ratio is measured. Temporal structure of filter is proposed which maintain constant SNR irrespective of distance. Remarkable development was achived. The method required prior knowledge of scene geometry. Low spatial frequency information also restored. This method was the first research work on image formation inverse model to restore visibility, but requires multiple images.**Tan** [4] in 2008: single image dehazing based on two prior knowledge assumptions, i) foggy image has less contrast than that of clear day , ii) object viewed from acquisition point exponential ly decays due to airlight and makes distant object smooth and invisible due to the presence of parti cles in the atmosphere those absorb and scatter light which was modeled by linear combination of direct attenuation and airlight . The main advantage was automated system and the requirement of single image without any geometrical information which made the method unique. A Markov ran dom field based cost function efficiently optimized by belief propagation or graph-cut has been de veloped. The method is efficient as required single image, but not applicable for real time. The method suffers from "halo" effect due to abrupt depth change which leads to colour over-saturation. Fattel [5] in 2008: Research work of R Fattal based on single image haze, and scatter light estima tion. From that information haze free image contrast has been recovered to increase visibility. It has been assumed that transmission and surface shading is locally uncorrelated. This simple statistical assumption reduces other complexity like surface albedo. The challenge of this method is to solve the pixels where no transmission is available. Implicit graphical model made it possible to extrapo late solution of those pixels. R Fattal estimated transmission map to get haze free image from single image. Scattering light is eliminated to increase visibility. Here, a new optical model presented where ambiguity of data has been resolved by surface shading and transmission, those are locally statistically uncorellated which successfully remove haze layers and find out exact colour of haze. Finally, the technique finds the solution of reliable transmission. The algorithm still suffers from blurriness due to atmospheric scattering. **He** *et al.*'s [6]: In some research work DCP (dark channel prior) has been used which is a statistical prior on haze free images. . This prior indicates that in normal RGB image 75% pixels of any dark channel is zero where dark channel indicates the lowest intensities channel out of three RGB image channel. 90% pixels of that channel are below 25. However, the scenario drifts radically in case of degraded weather. That corresponds to high intensity of dark channel. It is due to atmospheric airlight which shifts the pixels intensity to very high value producing almost white image. The method is efficient, but takes long time to reproduce due to its high computational complexity. Therefore, for real time application cannot be useful. He et al. came up a dark channel prior (DCP) technique which effectively trumps over other two techniques described above. In DCP, clear image contrast is high and pixel intensities distribute over the whole scale uniformly, whereas turbid weathered image, the intensities are not uniformly distributed, shift to upper side of the intensity scale and appear the image white. Under this assumption local patch with DCP is to identify and in turn transmission is estimated. Finally, image recovers using atmospheric scattering model as shown in equation (2). As already stated that in this scattering model, image is recovered by inversion which is compromised by some substantial blocking effect in the transmission map. Transmission map can be wisely estimated with sparing Laplacian ma-

trix. High Computational Complexity makes the technique not appropriate for fast operation. Still this method is quite satisfactory except dull output. **Tarel** *et al.'s* [7]: Fog, haze, smoke fade colour and contrast of outdoor images and make processing of those images difficult.The algorithm proposed

by J P Tarel is fast and its complexity is linear function with the number of image pixels applicable for both colour and gray single image. This is achieved by solving the problem of fog and low colour saturation objects assuming only small objects complemented with low colour saturation. Median filter is used to preserve edges which have less complexity and linear function with image size. Apart from that *median of median along lines filter* has been proposed to preserve edges as well as corners. The algorithm is tuned by only four parameters, atmospheric veil inference, image restoration, smoothing, and tone mapping. The technique is controlled by atmospheric veil inference, image restoration and smoothing, tone mapping. Qualitative and quantitative studies have been done extensively. **Berman** *et al.'s* [8]: Outdoor image often suffers from haze which reduce visibility and contrast. Furthermore, every pixel degrades differently depending from scene point to camera and this is expressed by transmission coefficients which is the reason for haze and attenuation. It is not a patch based prior contrary to previous methods. It is non-local prior. D Berman et. al. emphasised that degradation is not uniform. It is different for different pixels of the image and is controlled by transmission coefficient. It has been proposed colours of haze free image to be clus tered firmly and spread over the entire RGB image. These clustered colour pixels are non-local. These clustered pixels distributed differently depending on their different transmission coefficients. Whereas hazy image forms line of colours that was earlier clustered, called haze line. It recovers distance map and haze free image reproduce from haze line. The algorithm is linear, faster, deterministic, no training required. In [12] authors proposed three algorithms and revised DCP by gam ma correction, contrast controller, sky masking and guided filtering. In [13, 14, and 15] authors emphasised on objective evaluation of DCP method and mathematical modelling of image formation. DCP is basically patch based or local prior. Patch size in was 15x15, omega was 0.95. These two parameters play a significant role. This has been shown. DCP with sky masking is a useful algorithm. But the value of optimum value is difficult to find out. It is evaluated manually. In [13] this difficulty has been recovered by using Cuckoo Search Algorithm. Resultant image using CSA re moves the artifacts of sky reflection very well. Visibility Improvement is a classical Inverse problem. Haze is always associated with blurring. Here both have been treated and removed. Computational complexity is an integral part of any machine computing task. Effort has been given to reduce computational complexity for fast application with qualitative and quantitative analysis [15]. **Contribution**-So far authors are dealing with local and nonlocal patch or pixel based spacial visibility improvement of digital images. In this work, wavelet domain visibility improvement is experimented.

3. Image formation physics-based model, inversion, and noise

In prior knowledge-restoration based dehazing, reconstruction of original scene radiance is achieved through an inverse transformation mechanism. Degradation model, and Physics based optical scattering model are famously known image transformation model. They are shown respectively in figure 2 and figure 3.
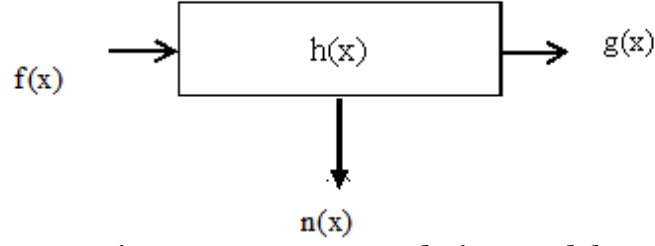
Figure 2. Image Degradation Model

Figure 2 shows degradation model where f(x) is the original scene radiance, g(x) is the degraded image, h(x) is the degradation function, and n(x) is the additive noise. Then, the linear time invariant system is represented by

$$g(x) = f(x)*h(x) + n(n) \tag{1}$$

a) Physical based optical scattering model:

This model is based on scattering principles of optics, more specifically Mie scattering, that was advocated by H Koscheder in 1924 and reinforced by McCartney [10,11]. In 1998 Okley et al. [9] used this model for the first time to improve image quality under poor visibility conditions. Since then this problem is rese arch hot spot. This model states that image captured by camera is divided into two parts, one is direct attenuation of light from scene radiance to the camera, and the other is scattering of airlight ending up at the camera. Thus the final image producing at the camera can be considered as blurry, low contrast, and poor visibility and noisy. This mechanism is described in figure 3,
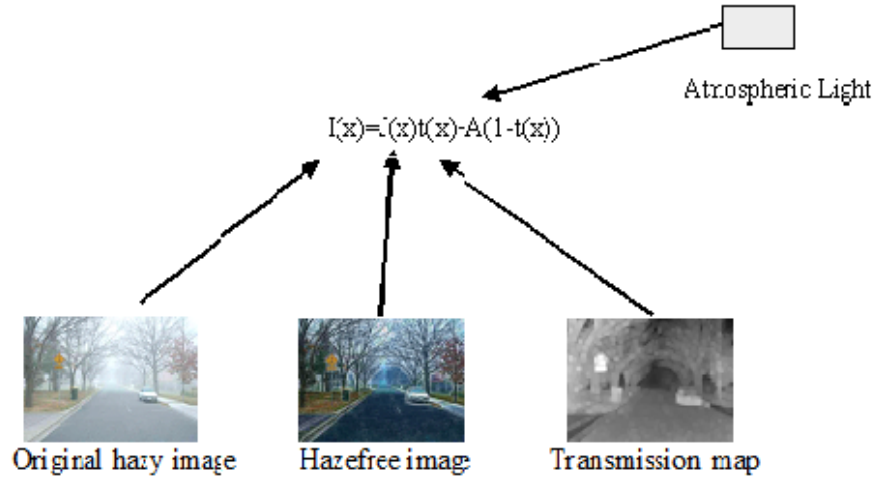
Figure 3 Image Formation Optical Model

Considering all the above constrains, atmospheric scattering model can be represented by

$$I(x) = J(x)t(x) + A(1 - t(x)) \tag{2}$$

where the first term I(x) is degraded image, J(x) represents original scene radiance/ image, t(x) is transmission map, and A as Atmospheric light. In equation 2, three variables are unknown. If t(x) and A could be estimated effectively, then J(x) could be recovered as close as original radiance. Thus, to recover J(x) is in verse problem. Therefore, it is evident that good or optimum estimations are the key to restore J(x). t(x) can be estimated from depth estimation, multiple images, or from some prior with single image. But estimation of the unknown parameters leads the overall problem as ill-posed inverse problem or constrain / intractable optimisation problem.
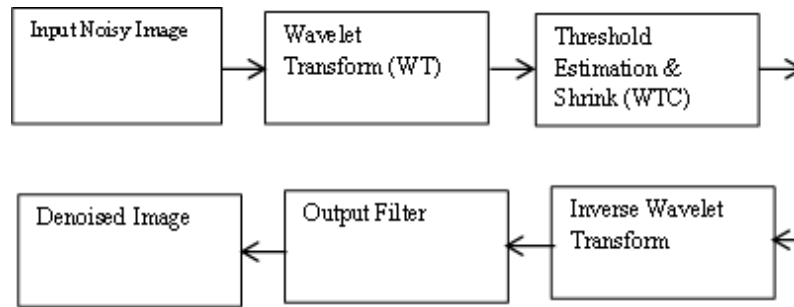
4. Wavelet Based Denoising Model

Fig 4 Block Diagram of Basic Denoising process

Wavelet transforms allows to display signals with a high degree of sparsity. wavelet denoising is a non-linear wavelet based signal estimation technique. Wavelet denoising attempts to remove the noise present in the signal while preserv ing the signal characteristics, regardless of its frequency content. It involves three steps: a linear forward wavelet trans form, nonlinear thresholding step and a linear inverse wavelet transform and shown in figure 4. Wavelet denoising must not be confused with smoothing; smoothing only removes the high frequencies and retains the lower ones. Wavelet shrinkage is a non-linear process and is what distinguishes it from entire linear denoising technique such as least squares. wavelet shrinkage relies heavily on the selection of a thresholding parameter and this selection of this threshold controls, to a great extent, the efficacy of denoising. Researchers have developed various techniques for choosing denoising parameters and so far, there is no "best" universal threshold determination technique [16]. **Biorthog onal spline Wavelet:** Orthogonal wavelet transforms are Haar, daubechies, Mordet, Mexican hat, Meyer, Symlet, Coiflets. They are of great use in different types of image processing applications widely. But, the said wavelets are notoriously known for false edge detection. In such situations, non-orthogonal specifically biorthogonal wavelet is desirable due to its flexibility and adaptability. Now, biorthogonal wavelet families are bior 1, 2,3,4,5, and 6 series and more. These series of biorthogonal wavelets are efficient to extract and restore geometric information of images those are acquired with projection, mix, and noise commonly. Classical derivative operators (Roberts, prewitt, sobel, LoG) do not works well due to false edge detection and their sensitivity to noise. These operators perform pixel wise which makes processing slow. The high frequency components consist of both edges as well as noise and in time domain it is absolutely difficult to solve. But, in case of orthogonal wavelets the problem is solved in different scale. As already explained that orthogonal wavelets are not also sufficient to detect edge. But, depending upon the properties and tuning of wavelets, like orthogonality, symmetry, and vanishing moments, good results of edge detection with geometry restoration can be achieved. Biorthogonal is the sure choice. Now according to human perception symmetric errors are better tolerant than asymmetric ones. Moreover, orthogonality and symmetry are two conflicting properties those have to trade off in case of robust edge detection. It is strictly maintained to be scaling functions to be symmetric for profound edge detection. Therefore, symmetric biorthogonal wavelets are the best choice. The orthogonal wavelets enjoy high degree of freedom with complex design issues, nonlinear phase analysis, synthesis filter bank and symmetric analysis capability only, here biorthogonal wavelets (nonorthogonal) present with more flexibility at the cost of energy partitioning. Spectral factorisation steps are also exempted from in case of biorthogonal filter which increases computational cost. Hear wavelet is the only orthogonal filter with symmetric, and finite length according to Daubechies. But shorter finite length prevents to detect large input change; therefore, length is to be considered greater than two with symmetric filter banks. Whereas in biorthogonal filer, both symmetric as well as asymmetric smooth design can be made possible. Multiresolution decomposition permits an image resolved into high quality attributes. Level 1 decomposition breaks an image into four subtends namely LL,

LH, HL, and HH. LL represents low resolution with low frequency components or average intensity, LH to horizontal details and shown in figure 5, HL for vertical details and HH for diagonal details of the image respectively. These subtends are the bases for MRA (Multi Resolution Analysis). With DWT the benefits are: dimensional reduction, less computational complexity, multiresolution data approximation, and insensitive feature extraction. DWT (Discrete Wavelet Transform) outperforms cosine transform, and Discrete Fourier transform. DWT is used for image analysis, compression, demonising due to its time and frequency domain representation simultaneously. Image can be decomposed into subtends by low and high frequency filters. They are LL, LH, HL, and HH. LL corresponds to upper left quadrant with all the coefficients with low pass filtering, LH to vertical edges in the lower left corner whereas HL for horizontal edges, in the vertical right corner and HH for high pass filtering in the lower right corner. This structure form 1-level decomposition. Now for 2-level decomposition LL from first level is again decom posed as I-level. But the LL of 2-level has half the height and width of previous level [17].

Popular Wavelet families

Table I. Popular wavelets and their families

Wavelet	Children	Short name
Haar	db1	haar'
Daubechies	db2, db3, db3, db4, db5, db6,db7, db8, db9, and db10	db'
Coiflets	1,2,3,4, and 5	coif'
Symlets	2,3, 4,5,6,7, and 8	sym'
Discrete Meyer		-
Biorthogonal	1.3, 1.5, 2.2, 2.4, 2.6, 3.1, 3.3, 3.7, 3.9, 4.4, 6.8	bior'
Reverse Biorthogonal		rbio'
Maxican Hat (Ricker Wavelet)		mexh'
Morlet		morl'
Complex Morlet		'cmor'
Gaussian Derivatives family		'gaus'
Complex Gaussian		'cgaus'
FIR based Meyer Wavelet		-
Complex Wavelet(Gaussian, Morlet, Frequency B-Spline, Shannon)		'cgaus', 'fmorl', 'fbspl', 'cshan'
Meyer Wavelet		'meyr'

Discrete approximation of Meyer wavelets		'dmey'
Shannon wavelets		shan'
Fejer-Korovkin		fk'
Frequency B-Spline		fbsp'

Thresholding of Wavelet coefficients: Most of the wavelet coefficients are zero or very low close to zero. By designing threshold more coefficients are forced to zero, so that sparsity will be created which leads to com pression as well as denoising. By product of this technique developed, easy manipulation of matrix inversion and computational complexity reduction can be achieved. In hard threshold is the tuning thresholding parameter which controls the thresholding by indulging coefficients below threshold to zero. Whereas in soft thresholding, same approach incorporated along with shrinkage of residual coefficients by subtracting the thresholding value λ. Now, the image matrix is compressed, noise free, as well as less space consuming that can be encoded and transmitted using entropy coding. In this work, we employ two types of thresholding, i) Brige-Massart Strategy, and ii) Unimodal Thresholding [18].
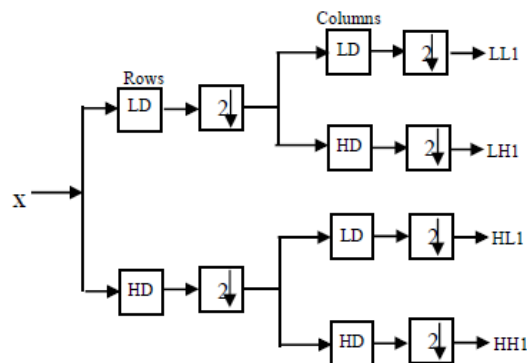
Fig 5 Filter Bank [19]
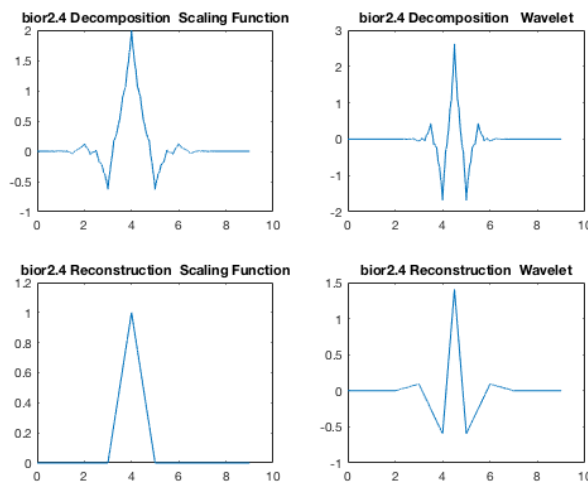
Fig. 6 Biorthogonal Wavelet
a). Bior2.4 decomposition scaling function, b) bior2.4 decomposition wavelet, c) bior2.4 reconstruction scaling function, d) bior2.4 Reconstruction wavelet

4.1 Birge-Massart Strategy for demonising (wavelet shrinkage) threshold with a tuning parameter of 3

This mechanism works as below: J0, m, and α are decomposition level, length of the coarsest approximation coefficient over 2, and real value greater than 1 respectively. For any level J, all coefficient values are kept for J0 +1 level. From the level 1 to J0, coefficient values are kept according to

$$k_j = \frac{m}{(J_0 + 1 - J)^\alpha} \tag{3}$$

Practical useful value of α is 1.5, and 1. Biorthogonal Birge-Massart Strategy for wavelet demonising is renowned for its noise removal from signal in wavelet domain without loss of important information specially edges in case of images. There is also almost no chance of false edge detection.

4.2. Wavelet Thresholding (shrinkage)

Introductory work of wavelet denoising with threshold was started by Donoho and Johnstone [21,22]. Image denoising with wavelet transform is efficient due to generation of a large number of small coefficients and a small number of large coefficients, from where noise coefficients can easily be deducted. Small coefficients are noise mostly, and large coefficients are information. Therefore, by thresholding with a proper value can reconstruct the original image without noise. Three basic steps of wavelet Denoising with thresholding: a. Wavelet transform of noisy image; b. Apply thresholding of noisy wavelet coefficients; c. Inverse wavelet transform on modified wavelet coefficients.
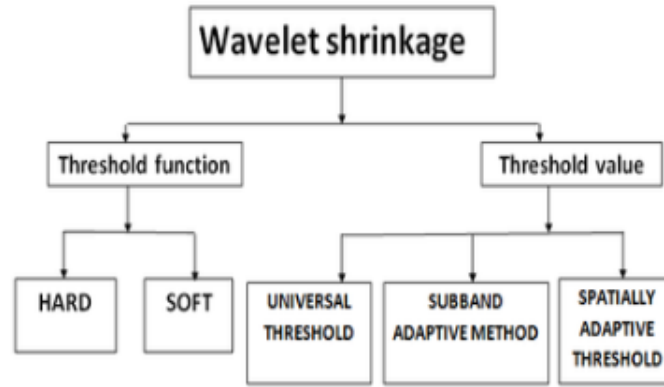
Fig 7 Wavelet thresholding (Shrinkage) and its different techniques [22].

Denoising process relies on thresholding. There are several techniques depending on threshold function and threshold values. Hard and soft threshold are two types of thresholding functions. Whereas, universal, subbed adaptive, and spatially adaptive thresholding are three types of thresholding dependent on threshold value.

4.2.1. Hard Thresholding

In hard thresholding, coefficients W_k are reset to zero whose value is less than a threshold value 'T' and others are remain W_k.

$$W_k = \begin{cases} W_k, for\ |W_k| \geq T \\ 0, otherwise \end{cases} \tag{4}$$
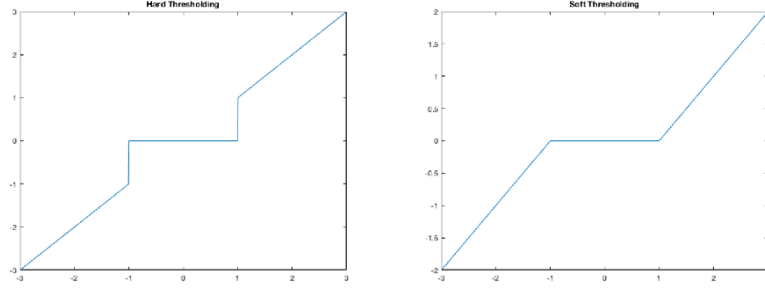
Fig 8 Right: Hard ThresholdingHard Thresholding, Right: Soft Thresholding

4. 2.2. Soft Thresholding

In soft thresholding, coefficients W_k are reset to zero whose value is less than a threshold 'T' and others are replaced by absolute value of (W_k- T).

$$W_k = \begin{cases} sgn(W_k)(W_k - T), for\ |W_k| \geq T \\ 0, otherwise \end{cases} \tag{5}$$

sgn(.) is signum function. It has been observed that soft thresholding is more efficient than hard thresholding, except few cases.

5 Application of Biorthogonal Birge-Massart Strategy for wavelet demonising in Image Formation Model

Reconstructed image comprises both intrinsic and extrinsic noise. Extrinsic noise causes transmission loss which makes the output image depthless and hazy and intrinsic noise is due to acquisition system inherent problem. Intrinsic noise is due to hardware design issues and is random in nature. Whereas extrinsic noise cane be modelled and removed. Good transmission could be retrieved from turbid transmission via approximate depth map (minimum intensity channel). Using this assumption transmission quality could be improved. Finer depth map is achiev**ed** by denoising through Biorthogonal Birge-Massart Strategy. As already discussed, Biorthogonal Birge-Massart Strategy denoised in sparsity controlled manner and edges are recovered with no false edge detection. . High frequency as well as low fre quency noise are removed by thresholding and decomposition level.Equation (6) is the optical physics based image degradation model that has been used in this paper[1,2]. Transmission has been predicted from equation (7). I(x), J(x), t(x), and A are degraded image, original image, transmission and atmospheric light respectively, β and d are extinction coefficient and distance respectively.

$$I(x) = J(x)t(x) + A\big(1 - t(x)\big) \tag{6}$$

$$t = e^{-\beta d} \tag{7}$$

During the transmission from original scene point to acquisition point, each pixel gets corrected with additive as well as multiplicative noise. This noise shifts colour, contrast, brightness, and sharpness of the pixel, and makes the result ing image whitish and almost invisible. When resource is single image, then it becomes difficult to tackle the problem. Therefore, minimum of three RGB -channel is considering depth map [12,13] and refinement is done using Lo-Gradi ent optimisation on that to get noiseless output which will produce clear transmission estimation. This is shown in equation (8), (9), and (10).

$$I_{cmin}(x) = \left(\min_{c \in \{r,g,b\}} (I^c(x) \right) \tag{8}$$

I^c and I_{cmin} indicate individual channel of RGB image and minimum of three channels I^c respectively. Noise that is found in the minimum intensity channel Icmin can now be used as raw depth map to recover haze free image and easily be made noise free or smoothened with

Birge-Massart Strategy for demonising (wavelet shrinkage) threshold (BBMS) shown by equation (3).

$$I_{cminBBMS}(x) = BBMS(I_{cmin}(x)) \tag{9}$$

Equation (9) shows noise free minimum intensity channel or refined depth map. This channel is normalised. Compliment of this equation will produce maximum intensity channel with BBMS denoising to produce prominent image structure and reduced computational complexity. This is a great advantage. This maximum intensity channel will be applied as the transmission estimation t(x). This transmission is severely ill-posed in nature. With BBMS, well-posed and good quality haze-free image will be generated without losing important structure of the original image. To generate depth map by minimum patch estimation which is more accurate, but it was computationally expensive [7]. Whereas this proposed concept is computationally simple and easy to implement. For fast application this approximation can be useful without hampering visibility and represented by equation (10).

$$t_{new}(x) = 1 - kI_{cminBBMS} \tag{10}$$

t_{new}, k are refined transmission and a proportionality constant for aerial perspective respectively [35,36]. The value of k is between 0 to 1. Zero indicates clear visibility like clear day scene, whereas one indicates absolutely no visibility like thick fog. The concept of k, haziness factor, will be discussed in detail [7,12,13].
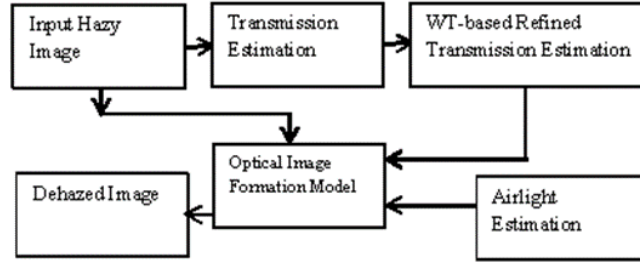
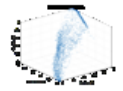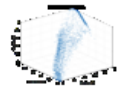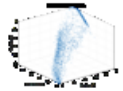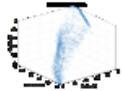Fig 9 Block Diagram of Biorthogonal Wavelet-based Visibility Improvement
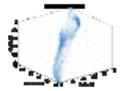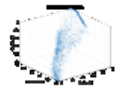
6 Experiment and Results

In order to verify the applicability and efficiency of the proposed dehazing method, we analyse it on various hazy , degraded, indoor, outdoor images and compare with Tan [4] , Fatal [5], He et al.'s [6], Tarel et al.'s [7], Nishino et al.'s [25], and Meng et al.'s [26], Q Zhu et el.'s [27], W Red et al.'s [24] , D Berman et al.'s [28] methods. All the algorithms are on the MatlabR2018a environment on a MacBook AirP4-, 1.8 GB 1600MHz DDR3, Graphics 6000 1536 MB. Popular wavelets have been given in Table I. These wavelets are being used to improve depth map of image formation model eq(6,10) by reducing noise .

6.1 Visual Appraisal of Proposed Technique with different wavelets/ Subjective Evaluation of Various Methods on

A hazy image from [6] dataset has been used for effectiveness test (both qualitative and quantitative) of the proposed algorithm in Table II. 'haar,' 'db3',' sym2', 'bior1.3', 'bior2.4' wavelets with level 5 are implemented in the depth map information which in turn produces refined transmission estimation for effective visible images. Finally, original scene radiance is well approximated with optical image formation model. The results show that all wavelets are appropriate for recovering original clear image. But bior1.3 and 2.4 showing little better result than the others. In case of computational complexity, db3 is slightly more efficient than the others marginally.

Table II. Effect of different wavelets on the same image using the proposed technique

Wave-let Type	Original Image	Level 5				
		Haar	**Db3**	**sym2**	**Bior1.3**	**Bior2.4**
Image						
Edge Pixel Detect-ed	-	2449	2461	2456	2463	2478
Ratio of Edge point	-	97.96%	98.4400	98.2400	98.5200	99.1200
PSNR	-	14.6713	14.7409	14.7121	14.7410	14.8441
SSIM	-	0.7230	0.7291	0.7275	0.7251	0.7391
Com-puta-tion Time	-	0.292830	0.283426	0.286624	0.307898	0.290957
3D plot						

Several state-of-the art algorithms along with proposed one have been designated to perform quality and quantity analysis in figure 10 with four images from [24,28], Indonesia.png, hazy day.png, swan.jpg, woman.png. Actual subjective assessment is too complicated and time consuming [29]. So here image visual quality is considered as subjective assessment. First three images of figure 10 have sky area. The proposed technique removes haze efficiently with no halo effect which is a extreme challenge for any dehazing, defogging or any deblurring technique with sky area. It is clear from the comparative quality of the other state-of-the art techniques that the proposed method is no lesser efficient than others. Lastly, the fourth image is a closer view of woman face. The proposed technique outperforms other techniques from the visual appearance. All the four images with the said technique are rich in colour, well contrast, no halo effect (especially in the sky area), and no colour dispersion.
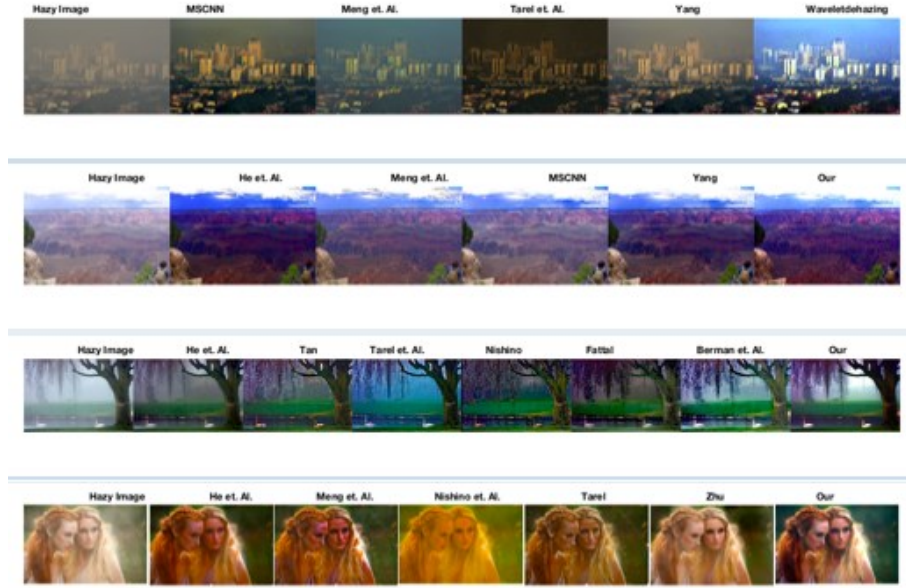
Figure 10 Proposed technique with other methods a comparative analysis, Top row: Indonesia.png, second row: Hazy Day.png, third row: Swan.png, Bottom row: Woman.png

6.2 Objective Analysis of Various Methods

As already mentioned, subjective assessment is happened to be biased. The objective IQA are very important and objective IQA employed here are SSIM, entropy, compression ratio, PSNR, MSE as full reference image metric and NIQE (Natural Image Quality Evaluator) [30] and BRISQUE(dubbed blind/reference less image spatial quality evaluator) [31]as no reference image metric/ blind or reference less IQA.No-reference algorithms compare statistical features of the input image against a model trained with a large database of naturally acquired images, whereas full reference image metric compares with respect to a known reference , ground truth or corrupted image .MSE measures the average squared difference between actual and ideal pixel values. This metric is simple to calculate but might not align well with the human perception of quality. Peak signal-to-noise ratio (PSNR) is derived from the mean square error, and indicates the ratio of the maximum pixel intensity to the power of the distortion. The PSNR metric is easy to calculate but might not align well with perceived quality. Structural Similarity (SSIM) Index metric merges local image structure, luminance, and contrast into a single local quality score. The SSIM quality metric is closer to the subjective quality score due to the high ability of human visual system for perception of visual structure. Blind IQA evaluates the quality of image without prior knowledge or reference image. This metric compares the image under examination with a set of trained images [30,31]. BRISQUE metric is operated on spatial domain. This metric examines naturalness of the said image with respect to trained on a database of images with known distortions. BRISQUE is limited to evaluating the quality of images with the same type of distortion. BRISQUE is opinion-aware, which means subjective quality scores accompany the training images. NIQE depends on the construction of a "quality aware" collection of statistical features of a simple and successful space domain natural scene statistic (NSS) model. NIQE can measure the quality of images with arbitrary distortion. NIQE is opinion-unaware, and does not use subjective quality scores. The no-reference algorithms calculate the quality score of an image with computational efficiency after the model is trained. Both no-reference quality metrics usually outperform full-reference met rics in terms of agreement with a subjective human quality score. These objective IQAs are listed in table III with image woman.png as the input from figure 10. Its graphical representation is shown figure 11. The outcome of objective tests revel that presented technique produce good results as compared with state-of -the art techniques.

Table III Objective Assessment an image woman.png as in fig 10.

Parame-ter	woman_input.png	He	Meng	Nishino	Tarel	Zhu	Our
Full Reference Image Quality Metric							
SSIM	-	0.6007	0.6802	0.5264	0.6557	0.7414	0.5970
Entropy	7.5549	7.3922	7.3745	5.9013	7.4074	7.6795	7.4929
Compression Ratio	1.0000	0.9630	0.9912	0.6958	0.9876	0.9918	1.0017
PSNR		10.0795	10.7039	10.9502	10.5577	12.9210	13.1814
MSE		638.45	5529.6	5224.6	5718.9	3318.8	3125.6
No Reference Image Metric							
NIQE	4.6505	4.2741	3.8480	3.9073	4.9527	3.5181	4.6358
BRISQUE	37.5996	37.6885	38.9087	34.4576	42.2790	34.5720	30.2550
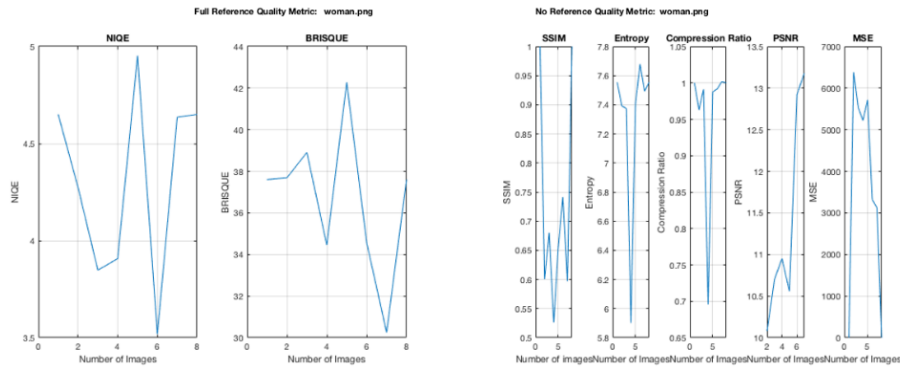
Figure 11. Graphical Objective evaluation of woman.png of fig 10 using table III

6.3 Effect of penalising tuning parameter Alpha (2-10)

The range of penalising tuning parameter Alpha, a real number, is (2-10), and its value greater than 1 (one) is pre ferred. Alpha is a tuning parameter responsible for sparsity (both compression and denoising). As alpha increases spar sity also increases. Apart from that for compression alpha is 1.2 and for denoising greater than 2 is favoured.The tech nique based on three parameters: a. the level of decomposition J, b. a positive constant M, and c. a sparsity parameter 'α'. Here, all approximation coefficients are at the decomposition level J. Further-more, at each decomposition level i, highest coefficient ni is kept and is represented by

$$n_n = \frac{m}{(J + 2 - i)^\alpha} \tag{11}$$

The threshold value is decided through mathematical model as:

$$T = \sqrt{\log(n)}$$

n is the length of the signal and σ² is the estimated noise variance. Sparsity parameter a keeps the value 1.2 for com pression and M is a wavelet coefficient dependent length parameter L. where, a is sparsity parameter , greater than 1, M is the detail wavelet coefficients , sorted in descending order of their absolute values, σ² is the noise variance, Now, a , the sparsity pa-rameter, is also known as penalising parameter, and the choice of the penalising value is pro-

posed as   penalising high 2.5< a<10, penalising medium 1.5<a<2.5 , and penalising low 1<a<2 .This is shown in the table IV below.
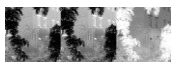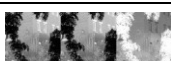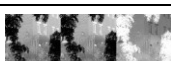
Table IV: M vs. Score of L

Score	M value
High	L
Medium	1.2*L
Low	2*L

In table v, it has been shown that sparsity increases as the penalising parameter alpha increases which leads to lowering complexity.

Table V Increasing alpha provides more sparsity in the result which leads to less complexity.

Alpha	Depth Map Transmission Map	Bior2.4 Dehazed Image	PSNR	SSIM	% Edge detected
1.2(compression)			16.2495	0.9974	17.4791
2			16.2308	0.9974	17.8763
3			16.2125	0.9974	18.8988
4			16.1966	0.9974	19.4165
5			16.1837	0.9974	21.7284
6			16.1727	0.9974	23.4346
7			16.1614	0.9974	24.2193
8			16.1514	0.9974	25.5348
9			16.1427	0.9974	28.7519
10			16.1335	0.9974	27.9900

6.4 Experiment with different thresholding value

Fig 12 a Hard Threshold 1.2-10, Top: Depth map, Middle: Transmission Estimation, Bottom: Recovered output

Fig 12 b Soft Threshold 1.2-10, Top: Depth map, Middle: Transmission Estimation, Bottom: Recovered output

Table VI. Experiment of Soft or hard threshold with bior2.4
Parametric evaluation of Soft and hard threshold with bior2.4. (Thresholding range 1.2-10)

Thresholding	PSNR	SSIM	% Edge detected	Entropy of dehazed image(original image Entropy= 7.35358897939924)	Compression Ratio
Hard Thresholding					
α= 1.2	17.6670	0.9979	1.4241	7.5613	1.000
α= 2	17.6317	0.9979	1.8517	7.56683	0.9999
α= 3	17.5900	0.9979	3.5475	7.57083	0.9998
α= 4	17.5481	0.9979	3.7033	7.57404472480660	0.9997
α= 5	17.5069	0.9979	5.0549	7.57683913149836	0.9996
α= 6	17.4707	0.9979	7.2617	7.579414	0.9995
α= 7	17.4413	0.9979	8.4683	7.581756	0.9995
α= 8	17.4140	0.9979	10.6243	7.58453	0.9994
α= 9	17.3900	0.9979	11.3636	7.58613	0.9993
α= 10	17.3666	0.9979	11.4252	7.5881	0.9992
Soft Thresholding					
α= 1.2	17.4012	0.9979	14.3421	7.5864	0.9995
α= 2	17.3156	0.9979	18.0998	7.5957	0.9990
α= 3	17.2329	0.9979	21.2849	7.6016	0.9985
α= 4	17.1665	0.9979	23.5279	7.6059	0.9982
α= 5	17.1111	0.9979	25.9014	7.6096	0.9978
α= 6	17.0636	0.9979	26.7130	7.6123	0.9975
α= 7	17.0219	0.9979	16.7156	7.6146	0.9972
α=8	16.9844	0.9979	19.0528	7.6167	0.9969
α= 9	16.9503	0.9979	19.6978	7.6184	0.9966
α= 10	16.9189	0.9978	20.7921	7.6199	0.9963

In table VI, gugong.bmp [7] has been experimented for thresholding. Wavelet bios 2.4, level 5 is used for set up environment. Hard and soft thresholding are operated on the image. PSNR, SSIM, % of edge detected, entropy, and com pression ratio have been used for parametric evaluation. These parameters are plotted for soft thresholding and hard thresholding in figure 11 and 12 respectively. From the figure it is shown that for hard thresholding optimum result is achieved around (4-5) when

Fig 13 a) Top Left: Hard Threshold vs. PSNR, b) Top Middle: Hard Threshold vs. SSIM, c) Top Right: Hard Threshold vs. % of edge detected, d) Bottom Left: Compression vs. Hard Threshold, e) Bot tom Middle: Entropy vs. Hard Threshold, and f) Bottom Right: Compression Ratio vs. PSNR.
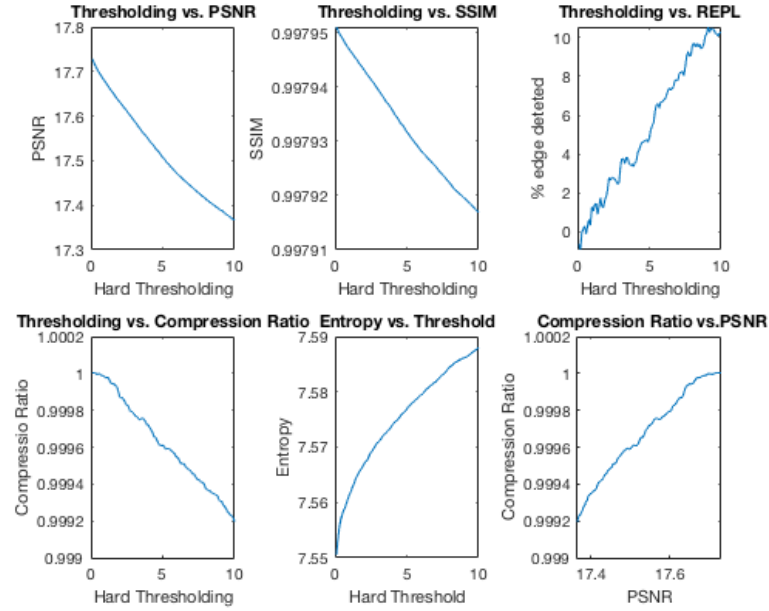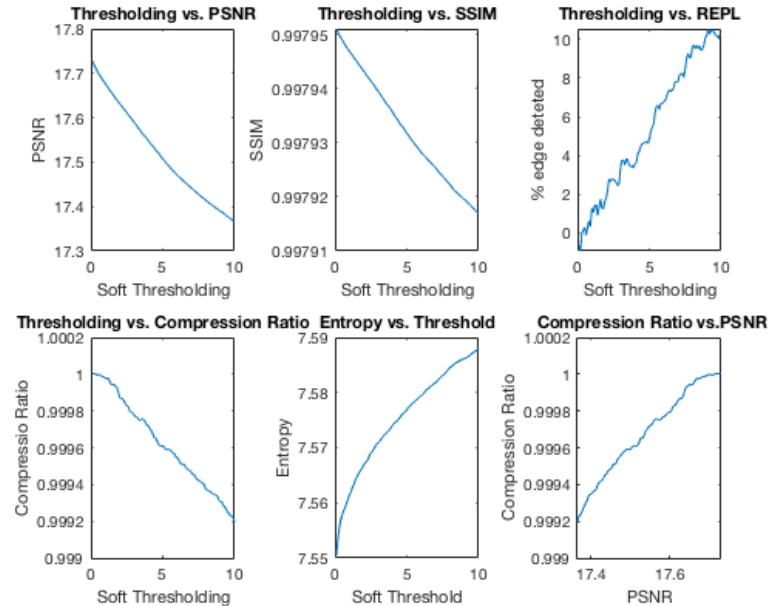

Fig 14 a) Top Left: Soft Threshold vs. PSNR, b) Top Middle: Soft Threshold vs. SSIM, c) Top Right: Soft Threshold vs. % of edge detected, d) Bottom Left: Compression vs. Soft Threshold, e) Bot tom Middle: Entropy vs. Soft Threshold, and f) Bottom Right: Compression Ratio vs. PSNR.

6.5 Time complexity:

It is the characteristics of an algorithm used. For any algorithm the most desirable criterion is efficiency, how much time and memory is utilised to perform a task in terms of seconds and megabytes respectively. But this is not a subjective assessment, because of its dependency on computational machine and data set used [16]. Wavelet Transform is an efficient mathematical tool. Discrete Wavelet Transform (DWT) has linear computational complexity of $O(n)$ which makes DWT fast. Most of the wavelet coefficients are sparse. Some DWT, like BWD, has complexity of $O(n \log_2 n)$ [20, 23]. Therefore, the table VII shows that the proposed technique has a complexity of $O(n \log_2 n)$.

Table VII Time / computational complexity of **Proposed Algorithm**

Algorithm	Input Hazy Image	Computational Complexity
Step I	Average of minimum of three channels as I_{min}	$O(n)$
Step II	Average of maximum value of three channels as I_{max}	$O(n)$
Step III	Contrast value=$I_{max} - I_{min}$	$O(n)$
Step IV	Haziness factor, k =I_{min} / I_{max}	$O(n)$
Step V	Airlight Estimation	$O(n)$
Step VI	Estimation of minimum intensity channel	$O(n)$
Step VII	Refinement of minimum intensity channel by Biorthogonal Birge-Massart Strategy for wavelet demonising	$O(n \log_2 n)$ [23]
Step VIII	Transmission Estimation	$O(n)$
Step XI	Recovery of Dehazed image with image degradation model	$O(n)$

7. Application of Wavelet-based Dehazing on different degraded Images

Images with different degraded form like underwater, rain, close object, night-time, etc have been examined and found remarkable results. Therefore, this can be concluded that the proposed approach is equally applicable for any kind of degraded images as well.

Figure 15. Application of Wavelet Dehazing on different degraded images

8. Conclusion, shortcoming, and future scope

In this paper, a comprehensive report has been documented with comparative analysis of different state-of-the art im age de-hazing as well as visibility improvement due to heavy demand of this issue [1-11]. Images of day-time, night, under water, rainy, and close objects of different types of unclear scene with sever degradation of [6,24,28] and FRIDA data set used. H Kosmedier image formation physics model has been deployed to solve the dehazing problem along with Biorthogonal Birge-Massart Strategy for wavelet demonising in transmission estimation stage as atmospheric light and transmission are the key parameters governing the haze removal. Depth map has been extracted by the mini mum intensity of 3-RGB channels with Biorthogonal Birge-Massart Strategy for wavelet demonising in sparsity-controlled manner. This in turn prod uses optimum transmission that leads to final resulting clear image. This technique is equally applicable for gray as well as colour image Dehazing. A set of wavelet functions (wavelets) with thresholding parameter (hard, soft) has been tuned from 1 to 10 grade and its effect has been observed where 1.2 thresholding value for the compression and higher value for demonising. The choice of optimal threshold has been observed for picture quality evaluation. Subjective evaluation is performed with visual assessment of recovered imaged with state-of-the art techniques. PSNR, SSIM, %edge detected, and entropy have been adopted for objective evaluation. Subjective and objective evaluations show satisfactory results. To minimise time complexity is a major limitation for any real time ap plications. Here, in this algorithm we tried to overcome the issue by BWD which has low computational complexity with high efficiency. Therefore, by observing and analysing the resulting images, this can be inferred that all types of unclear images are equally recovered their visibility with this algorithm. A powerful-principled, fast, and pertinent algorithm has been presented with well contrast, no colour dispersion, and halo free image. There is a wide scope for recovering good quality image in future with the advancement of low-cost camera technology and computational pro cessing. In future this method can be applied with some modification in other demonising and deblurring problems. Another vital application area is to estimate depth for semantic segmentation, object detection in vision task where ground truth depth dataset is unavailable.

References

1. Sung Cheol Park, Min Kyu Park, and Moon Gi Kang, Super-Resolution Image Reconstruction: A Technical Over view, IEEE Signal Processing Magazine, May 2003. 1053-5888/03/$17.00©2003IEEE.

2. Yoav Y. Schechner, Member, IEEE, and Yuval Averbuch, Regularized Image Recovery in Scattering Media, IEEE Transactions on Pattern Analysis and Machine Intelligence, Vol. 29, No. 9, September 2007.

3. W. Wang, X. Yuan, Recent Advances in Image Dehazing, IEEE Journal of Automatica Sinica, Vol. 4, No. 3, July 2017.

4. R Tan, Visibility in Bad Weather from A Single Image, 2008 CPVR, IEEE Explore, DOI: 10.1109/CVPR. 2008.4587643, ISSN: 1063-6919.

5. R Fattal, Single Image Dehazing, ACM Transaction on Graphics(TOG), vol-27, Issue-3, August2008.

6. K.,He, J., Sun, and X., Tang,: Single image haze removal using dark channel prior", IEEE Conference on Computer Vision and Pattern Recognition, Miami, FL, 2009,pp- 1956 – 1963.

7. J. P. Tarel, Hautiere, N., Fast visibility restoration from a single color or gray level image, IEEE 12th International conference on Computer Vision (2009) 2201 – 2208.

8. D Berman, T Treibitz, S Avidan, Non-local Image Dehazing, CVPR2016.

9. J. P. Oakley and B. L. Satherley, "Improving image quality in poor visibility conditions using a physical model for contrast degradation," IEEE Trans. Image Process., vol. 7, no. 2, pp. 167°179, Feb. 1998.

10. H. Koschmieder, Theorie der horizontalensichtweite, Beitr.Phys. Freien Atm., vol. 12, 1924, pp. 171–181.

11. E J McCartney, Optics of the Atmosphere: Scattering by Molecules and Particles, New York, NY, USA:Wiley, 1976.

12. D Das, S Roy, S S Chaudhuri, Dehazing Technique based on Dark Channel Prior model with Sky Masking and its quantitative analysis, CIEC16, IEEE Explore, IEEE Conference ID: 36757.

13. S Roy, S S Chaudhuri, Modelling and control of sky pixels in visibility improvement through CSA, IC2C2SE2016.

14. S Roy, S S Chaudhuri, Modeling of Ill-Posed Inverse Problem, IJMECS, 2016, 12 pp-46-55.

15. S Roy, S S Chaudhuri, Low Complexity Single Colour Image Dehazing Technique,Intelligent Multidimensional Data and Image Processing, June 2018, IGI Global.

16. Image Denoising Using Wavelets, — Wavelets & Time Frequency —, Raghuram Rangarajan Ramji Venkatara manan Siddharth Shah, December 16, 2002.

17. Siraj Sidhik, Comparative study of Birge–Massart strategy and unimodal thresholding for image compression us ing wavelet transform, OPTIK, ELSEVIER, 2015, Optik 126 (2015) 5952−5955.

18. Wavelet Signal and Image Denoising, E. Hostalkova ´, A. Prochazka,Institute of Chemical Technology Department of Computing and Control Engineering.

19. Comparative Analysis of Filters and Wavelet Based Thresholding Methods for Image Denoising, Anutam, Rajni, SBSSTC, SBSSTC, Ferozepur, Punjab.

20. Discrete Wavelet Transform Decomposition Level Determination Exploiting Sparseness Measurement, Lei Lei, Chao Wang, X Liu, World Academy of Science, Engineering and Technology International Journal of Electrical and Computer Engineering Vol:7, No:9, 2013.

21. D. L. Donoho and I. M. Johnstone, −Adatpting to unknow smoothness via wavelet shrinkage, ‖ Journal of the American Statistical Association, vol. 90, no. 432, pp. 1200-1224, December 1995. doi:10.1.1.161.8697.

22. A Dixit, P Sharma, A Comparative Study of Wavelet Thresholding for Image Denoising, I.J. Image, Graphics and Signal Processing, 2014, 12, 39-46, DOI: 10.5815/ijigsp.2014.12.06.

23. H Guo, C S Burrus, Fast Approximate Fourier transform via Wavelets Transform, Proceedings of the SPIE, Vol ume 2825, p. 250-259 (1996).

24. W Ren, S Liu, H Zhang, J Pan, X Cao, M-H Yang, Single image dehazing via multi-scale convolutional neural Networks, European conference on computer vision,Springer, Cham,October2016, pp.154-169.

25. L. Kratz and K. Nishino, "Factorizing scene albedo and depth from a single foggy image," in Proc. IEEE 12th Int. Conf. Comput. Vis. (ICCV), Sep./Oct. 2009, pp. 1701−1708.

26. Gaofeng MENG, Ying WANG, Jiangyong DUAN, Shiming XIANG, Chunhong PAN, Efficient Image Dehazing with Boundary Constraint and Contextual Regularization ,2013 IEEE International Conference on Computer Vision, 1550-5499/13 $31.00 © 2013 IEEE, pp.617-624.

27. Q Zhu, J Mai, L Shao, A Fast Single Image Haze Removal Algorithm Using Color Attenuation Prior, IEEE Transactions on Image Processing, Vol. 24, No. 11, November 2015, pp.3522-3533.

28. Dana Berman, Tali Treibitz, Shai Avidan, Non-Local Image Dehazing, IEEE, (CVPR2016), pp.1674-1682.

29. Pedram Mohammadi*, Abbas Ebrahimi-Moghadam*,1, and Shahram Shirani**, Subjective and Objective Quality As sessment of Image: A Survey', Majlesi Journal of Electrical Engineering, Vol. 9, No. 1, March 2015.

30. A Mittal, R Soundararajan, A C. Bovik, Making a "Completely Blind" Image Quality Analyzer, IEEE Signal Pro cessing Letters, Vol. 20, No. 3, March 2013.

31. A Mittal, A K Moorthy, A C Bovik, No-Reference Image Quality Assessment in the Spatial Domain,IEEE Transac tions on Image Processing, Vol. 21, No. 12, December 2012.

32. Roy, Sangita. "Single Image DnCNN Visibility Improvement (SImDnCNNVI)." Scientific Visualization 14.3 (2022).

33. Roy, Sangita, and S. S. Chaudhuri. "SIVDSR-Dhaze: Single Image Dehazing with Very Deep Super Resolution   Framework and Its Analysis." Scientific Visualization 14.5 (2022).

34. Roy, Sangita RLaMs-Dehazing: Optimized Depth Map Improvement Single Colour Image Dehazing, Scientific Visualization 15.4 (2023).